ISH Journal of Hydraulic Engineering

ISSN: 0971-5010 (Print) 2164-3040 (Online) Journal homepage: http://www.tandfonline.com/loi/tish20

Boundary shear stress distribution for a converging compound channel

B. Naik & Kishanjit K. Khatua

To cite this article: B. Naik & Kishanjit K. Khatua (2016): Boundary shear stress distribution for a converging compound channel, ISH Journal of Hydraulic Engineering, DOI: 10.1080/09715010.2016.1165633

To link to this article: http://dx.doi.org/10.1080/09715010.2016.1165633

Published online: 09 Apr 2016.

http://dx.doi.org/10.1080/09715010.2016.1165633

Boundary shear stress distribution for a converging compound channel

B. Naik and Kishanjit K. Khatua

Department of Civil Engineering, National Institute of Technology Rourkela, Rourkela, India

ABSTRACT
The boundary shear force distribution in open channel flow is needed for various purposes such as the flow resistance relationship, for designing stable channels. During floods, river overtops the main channel and flows over the flood plain located to its sides. For such compound channels the flow structure becomes complicated due to the transfer of momentum between the deep main channel and the adjoining flood plains that magnificently affects the shear stress distribution in flood plain and main channel subsections. Due to the rapidly growing population and the consequent demand for food and accommodation, more and more land on floodplain regions of a river system has been used for agriculture and settlement. This also causes flood plain geometry to vary along the length of the flow called converging compound channel. In this paper an experimental investigation concerning the distribution of shear stress in the main channel and flood plain of the converging compound channels are presented. Based on the experimental results of boundary shear, a new equation is developed for predicting boundary shear stress distribution in terms of non-dimensional geometric and flow variables.

ARTICLE HISTORY
Received 4 May 2015
Accepted 10 March 2016

KEYWORDS
Compound channel; boundary shear; discharge; divided channel method; non-dimensional flow parameters

1. Introduction

Accurate determination of the distribution of boundary shear stress on and near the banks of natural channels is essential for addressing a variety of problems in fluvial geomorphology and stream restoration. So it is very essential to study the flow mechanism of rivers both in in-bank and overbank conditions due to the velocity difference between the main channel and flood plains. Sellin (1964) first investigated through laboratory investigations the momentum transfer phenomena. After that several investigators found that the momentum transfer was responsible for the non-uniformity in the boundary shear stress distribution across the section perimeter (e.g. Ghosh and Jena (1971), Knight and Hamed (1984), Patra et al. (2004). Knight and Hamed (1984) developed a model for boundary shear tress distribution of homogeneous compound channel of width ratio (α = flood plain width (B)/main channel width (b)) value up to 4. Khatua and Patra (2007) based on more experimental observations carried forward the study and developed a model for channels of width ratio (α) value up to 5.25. Mohanty and Khatua (2014) again developed a new model for channel with $6.67 \le \alpha \le 11.96$. Both prismatic and meandering compound channels' geometries were extensively investigated in laboratory flumes. However, when the compound section data of prismatic compound channels were compared with non-prismatic compound channels significant errors in estimation of $\%S_{fp}$ were noticed due to non-inclusion of extra mass and momentum transfer as explained by Bousmar and Zech (1999), Bousmar et al. (2004), and Proust et al. (2006). Where $\%S_{fp} = 100 \times S_{fp}/SF$, S_{fp} = the boundary shear carried by the flood plains and SF the total shear force of the compound channel. This extra momentum exchange should be taken into account in the flow modeling for non-prismatic compound channel. Distribution of boundary shear stress mainly depends upon the shape of the cross-section and the structure of the secondary flow cells. So new models are necessary to be developed for the non-prismatic compound sections. New experiments on compound channels with converging flood plains were conducted to develop new expression for $\%S_{fp}$.

2. Experimental works

2.1. Experimental setup

Experiments have been conducted at the Hydraulics and Fluid mechanics Laboratory of Civil Engineering Department of National Institute of Technology, Rourkela, India. Three sets of non-prismatic compound channels with varying cross-sections were built inside a concrete flume with Perspex sheet measuring 15 m long × 0.90 m width × 0.5 m depth. The width ratio (α) of the channel was 1.8 and the aspect ratio (δ = main channel width (b)/main channel depth (h)) was 5. Keeping the geometry constant, the converging angles of the channels were varied as 12.38°, 9°, and 5°, respectively. Converging length of the channels fabricated were found to be 0.84, 1.26, and 2.28 m, respectively. Longitudinal bed slope of the channel was 0.0011, it was satisfying subcritical flow conditions at different sections of the non-prismatic compound channels. Roughness of the flood plain and main channel was taken identical. From the in-bank flow measurements of the channel of same surface materials (used in the main channel and flood plains) and using the back calculations of Manning's equations, Manning's n value of 0.011 has been estimated. The flow conditions in the converging section were turbulent. A recirculating system of water supply was established with pumping of water from an underground sump to an overhead tank from where water flows under gravity to the experimental channel. Adjustable vertical gates along with flow strengtheners were provided in

CONTACT B. Kishanjit banditanaik1982@gmail.com K. Naik Khatua kkkhatua@nitrkl.ac.in

upstream section sufficiently ahead of rectangular notch to reduce turbulence and velocity of approach in the flow near the notch section. An adjustable tailgate at the downstream end of the flume helps to maintain uniform flow over the test reach. Water from the channel was collected in a volumetric tank that helps to measure the discharge rate. From the volumetric tank water runs back to the underground sump. Figure 1a shows the plan view of experimental setup. Figure 1b shows the plan view of different test reaches with cross-sectional dimensions of both NITR & Rezaei (2006) channels. Figure 1c shows the typical grid showing the arrangement of velocity measurement points along horizontal and vertical directions at the test section.

A movable bridge was provided across the flume for both span wise and stream wise movements over the channel area so that each location on the plan of compound channel could be accessed for taking measurements. The broad parameters of this channel are aspect ratio of main channel (δ), width-ratio (α). A micro-Pitot tube of 4.77-mm external diameter in conjunction with suitable inclined manometer was used to measure velocity at these points of the flow grid. The Pitot tube was physically rotated with respect to the main stream direction till it gave maximum deflection of the manometer reading. A flow direction finder having a least count of 0.1° was used to get the direction of maximum velocity with respect to the longitudinal flow direction. The angle of limb of Pitot tube with longitudinal direction of the channel was noted by the circular scale and pointer arrangement attached to the flow direction meter. The overall discharge obtained from integrating the longitudinal velocity plot and from the volumetric tank collection was found to be within ±3% of the observed values. Using the velocity data, the boundary shear at various points on the channel beds and walls were evaluated from a semi log plot of velocity distribution. Boundary shear stresses were also obtained from the manometer readings of the head differences of Preston tube techniques using Patel's (1965) relationship. Error adjustments to the shear value were done by comparing the corresponding shear values obtained from the energy gradient approach. The results so obtained were found to be consistently within ±3% the value. According to the laboratory data analysis, shear stress from a Pitot tube is the most appropriate shear stress calculation method as compared to ADV. Because near the boundary velocity measurement ADV is never accurate. Further, ADV has some limitations of velocity measurements. It can measure 5 cm below its top edge. So in down probe of micro-ADV it

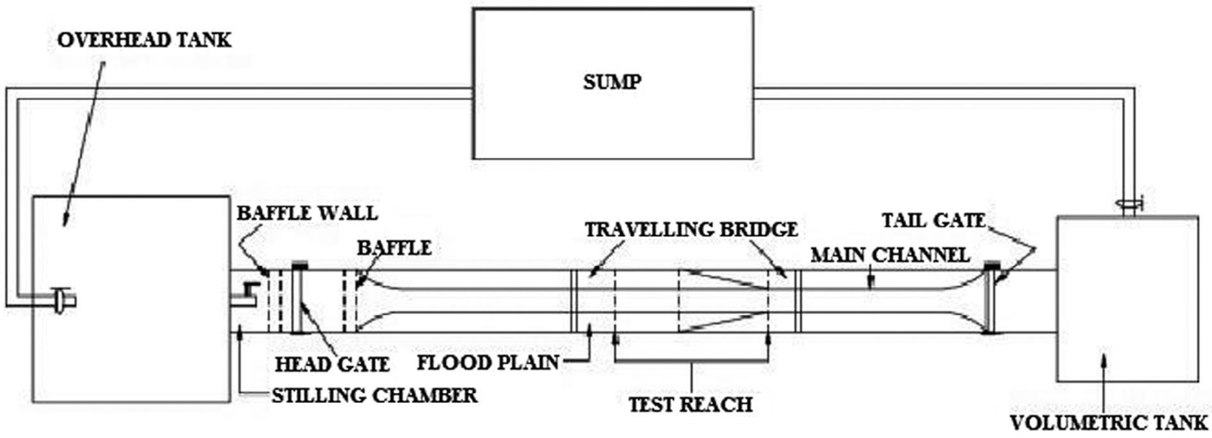

Figure 1a. Plan view of experimental setup.

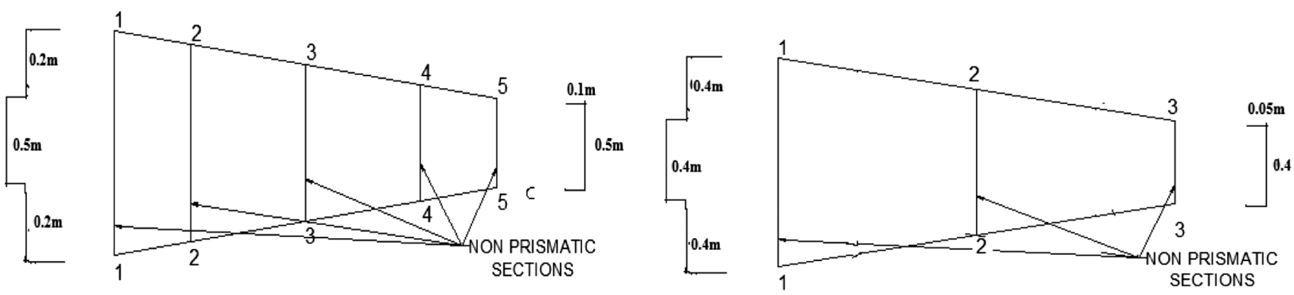

Figure 1b. Plan view of different test reaches with cross-sectional dimensions of both NITR & Rezaei (2006) channels.

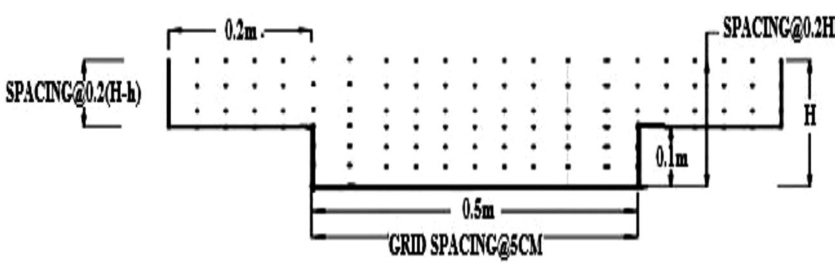

Figure 1c. Typical grid showing the arrangement of velocity measurement points at the test section.

could not measure 5 cm near the free surface. So Pitot tube has been utilized to measure the short fall. The accuracy of this method has been verified from the energy gradient approach i.e. weight component of the flow.

3. Experimental results

The results of boundary shear stress distributions for the converging flood plain of angle 12.38° and 11.31° of Rezaei (2006) for different cross-sections of relative depth 0.15 and 0.5 are shown in Figures 2a and 2b. These figures indicate that the boundary shear stress distributions are reasonably symmetric in all sections and gradually increase from sec-1 to sec-5. In all sections the boundary shear value is found to be the maximum at the middle of main channel and gradually decreases towards the interface between the main channel and the flood plain. At the interface, the boundary shear suddenly falls then it decreases and reaches the minimum at both the ends of flood plains. This may be due to momentum transfer phenomena between the main channel and flood plains. Similarly this happens to the converging channel of Rezaei (2006) with angle 11.31°. However, at the last section of Rezaei (2006) maximum boundary shear is found to occur at the two ends of the main channel instead of the middle of main channel. Because the last section is the single channel with higher aspect ratio as compared to the present experimental channel. To analyze the boundary shear stress distributions, various boundary elements of the non-prismatic compound channels comprising the wetted parameters are labeled as (1), (2), (3), and (4) as shown in Figure (3). Label (1) denotes the two vertical walls of flood plain of length [$2(H–h)$], and (2) denotes flood plain beds of length ($B–b$). Label (3) denotes the two main channel walls of length ($2h$) and the bed of the main channel of length b is represented by label (4) (where H is the total depth of the compound channel, h is the main channel height, and B is the total width of the compound channel). Experimental shear stress distributions at each point of the wetted perimeter are numerically integrated over the respective sublengths of each boundary element (l), (2), (3), and (4) to obtain the respective boundary shear force per unit length for each element. Sum

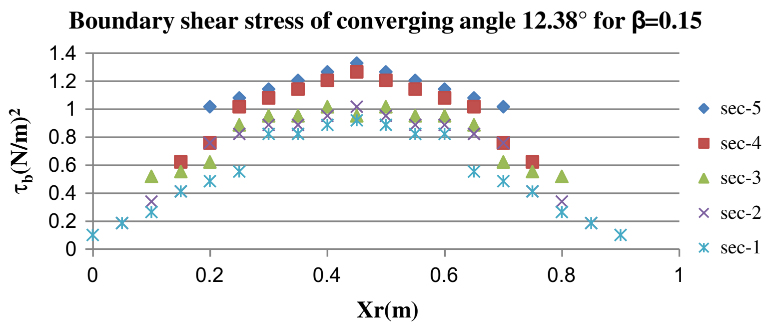

Figure 2a. Boundary shear distribution for the present experimental channel of relative depth 0.15 (for converging angle 12.38°).

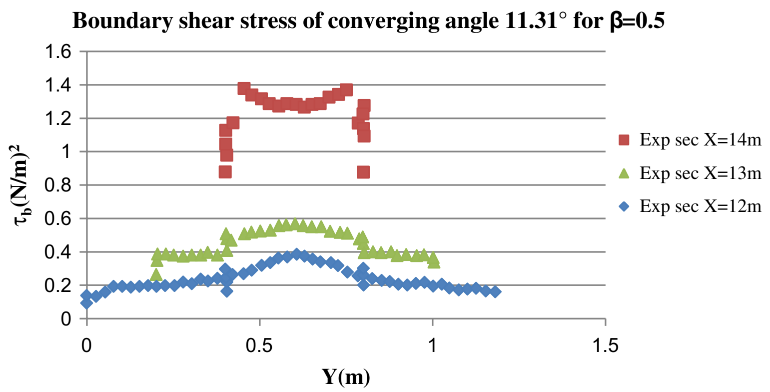

Figure 2b. Boundary shear distribution for the Rezaei (2006) experimental channel of relative depth 0.5 (for converging angle 11.31°).

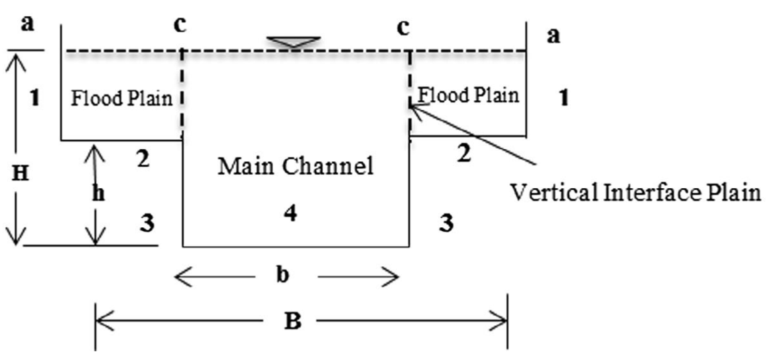

Figure 3. Interface planes dividing a compound section into subareas.

of the boundary shear forces for all the beds and walls of the compound channel is used as a divisor to calculate the shear force percentages carried by the boundary elements. Percentage of shear force carried by flood plains comprising elements (1) and (2) is represented as $\%S_{fp}$.

4. The boundary shear stress distribution model

In a simple open channel flow the boundary shear per unit length (SF) is generally assumed to be uniform and is expressed as $SF = \rho gAS$, where ρ is density of water and g is acceleration due to gravity. The parameters ρ, g, and S are assumed constant for a given channel. Only the flow area (A) varies with flow depth. So it can be stated that SF is a function of A. The percentage of the area occupied by the flood plain subsections obtained by vertical interfaces (Figure 3), is denoted by $\%A_{fp} = 100 \times A_{fp}/A$, where A_{fp} is the corresponding area by flood plain and A is the total area of the compound channel. Therefore, a functional relationship between $\%S_{fp}$ and $\%A_{fp}$ has been derived. This equation has been obtained by curve fitting between $\%A_{fp}$ and $\%S_{fp}$ which gave the highest regression coefficient. We have attempted to develop an equation of $\%S_{fp}$ with α and β for compound channels with converging flood plains. Previously different investigators have presented their model for $\%S_{fp}$. Knight and Demetriou (1983) presented an equation for the percentage of total shear force carried by the flood plain as $\%S_{fp}$

$$\%S_{fp} = 48(\alpha - 0.8)^{0.289}(2\beta)^{m} \quad (1)$$

where α = width ratio = B/b, β = relative depth = $(H–h)/H$, b = width of main channel, B = total width of compound channel, h = bank full depth, and H = total depth of flow. The exponent m is evaluated from the relation

$$m = 1/[0.75e^{0.38\alpha}] \quad (2)$$

Equation (1) is applicable for homogeneous compound channels. For non-homogeneous compound channels Equation (1) is improved by Knight and Hamed (1984) as

$$\%S_{fp} = 48(\alpha - 0.8)^{0.289}(2\beta)^{m}[1 + 1.02\sqrt{\beta}\log\gamma] \quad (3)$$

where γ = the ratio of Manning's roughness of the flood plain (n_{fp}) to that for the main channel (n_{mc}).

Equation (1) is good for $\alpha \leq 4$. Khatua and Patra (2007) further improved Equation (2) and proposed an equation for $\%S_{fp}$ as

$$\%S_{fp} = 1.23(\beta)^{0.1833}(38\text{Ln}\alpha + 3.6262)[1 + 1.02\sqrt{\beta}\log\gamma] \quad (4)$$

Khatua and Patra (2007) have shown the validity of Equation (4) for α up to = 5.25. Again for α = 6.67, Khatua et al. (2012) obtained a new relation for percentage shear carried by the flood plain as

$$\%S_{fp} = 4.1045(\%A_{fp})^{0.691} \quad (5)$$

In terms of β and α, Equation (5) is simplified as

$$\%S_{fp} = 4.105\left[\frac{100\beta(\alpha - 1)}{1 + \beta(\alpha - 1)}\right]^{0.691} \quad (6)$$

For width ratio up to 12, from regression analysis, Equation (5) is further modified by Mohanty and Khatua (2014).

$$\%S_{fp} = 3.3254(\%A_{fp})^{0.746} \quad (7)$$

Looking equations of different investigators i.e. Equations (1), (5), and (7) etc. it is seen that $\%S_{fp} = F(\alpha, \beta, \delta)$ for prismatic compound channel, where F is the functional symbol. But when all the equations are tested against compound channels with converging sections significant errors are found. So an attempt has been made here to investigate the variation in $\%S_{fp}$ with respect to different non-dimensional parameters of a non-prismatic compound channel. The percentage of shear carried by flood plain ($\%S_{fp}$) for non-prismatic sections have been derived from a wide range of experimental data-sets i.e. from three different types of converging compound channels of NIT, Rourkela, India and three series of converging compound channels data of Rezaei (2006) (details of the data-sets are given in Table 1). These compound channels have homogeneous roughness both in the main channel and flood plain subsections. Manning's n values for all these smooth surfaces are taken as 0.01. For a compound channel with converging flood plain the boundary shear distribution changes from section to section. So two additional parameters with the above three are considered for modeling of the boundary shear stress distribution of such compound channels. Therefore, a multiple variable regression model is attempted by taking all the five most influencing dimensionless parameters.

The possible functional relationships is in the form

$$\%S_{fp} = F\left(\alpha, \beta, \delta, \theta, X_r\right) \quad (8)$$

where θ = Converging angle, X_r = Relative distance (x/L), and L = Non-prismatic length.

The possible dependency of $\%S_{fp}$ and the best functional relationships with each non-dimensional variable have been found out from the Figures 4–6 described below. The variation in $\%S_{fp}$ has been plotted for six converging compound

Table 1. Hydraulic parameters for the experimental channel data.

Verified test channel	Types of channel	Angle of convergent (θ)	Longitudinal slope (S)	Cross-sectional geometry	Total channel width (B) (m)	Main channel width (b) (m)	Main channel depth (h) (m)	Width ratio (sec-1) B/b (α)	Converging length (X_r) (m)	Aspect Ratio b/h (δ)
Rezaei (2006)	Converging (CV2)	11.31°	0.002	Rectangular	1.2	0.398	0.05	3	2	7.96
Rezaei (2006)	Converging (CV6)	3.81°	0.002	Rectangular	1.2	0.398	0.05	3	6	7.96
Rezaei (2006)	Converging (CV6)	1.91°	0.002	Rectangular	1.2	0.398	0.05	3	6	7.96
N.I.T. Rkl	Converging	5°	0.0011	Rectangular	0.9	0.5	0.1	1.8	2.28	5
N.I.T. Rkl	Converging	9°	0.0011	Rectangular	0.9	0.5	0.1	1.8	1.26	5
N.I.T. Rkl	Converging	12.38°	0.0011	Rectangular	0.9	0.5	0.1	1.8	0.84	5

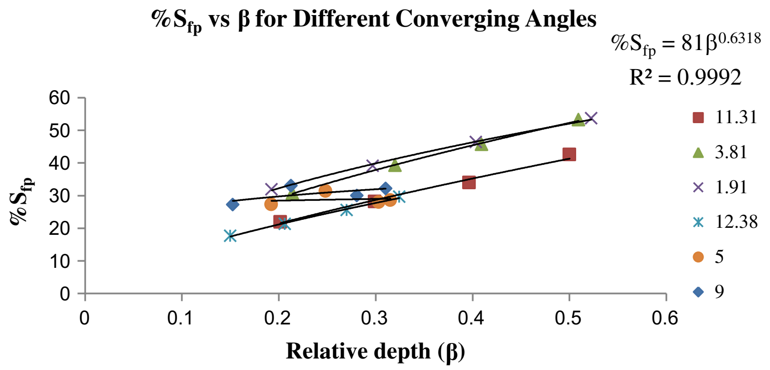

Figure 4. Variation in $\%S_{fp}$ of non-prismatic compound channel at typical sections.

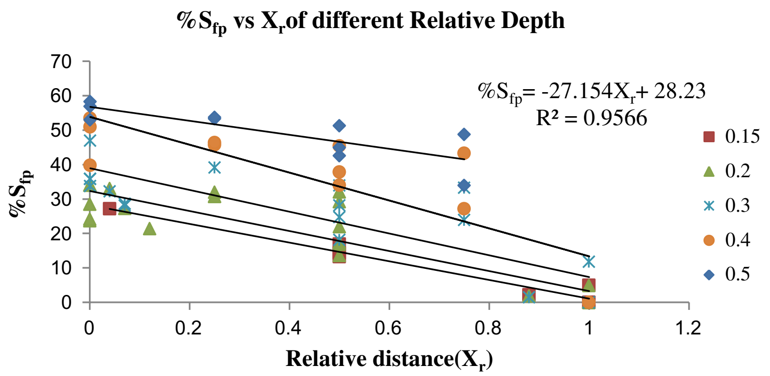

Figure 5. Variation in $\%S_{fp}$ of flood plain shear with section to section along the converging angle and prismatic channel width.

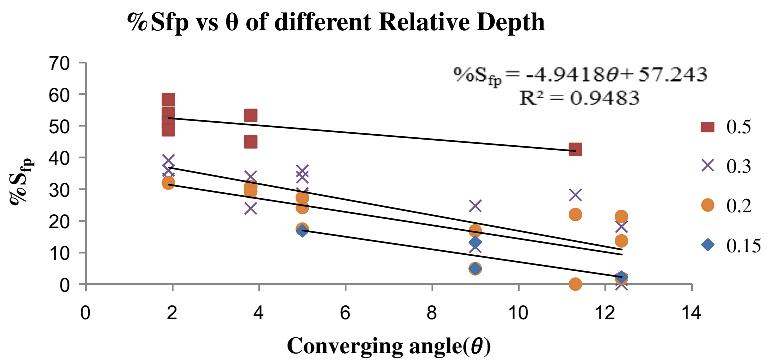

Figure 6. Variation in $\%S_{fp}$ of flood plain shear with converging angles for constant relative depth.

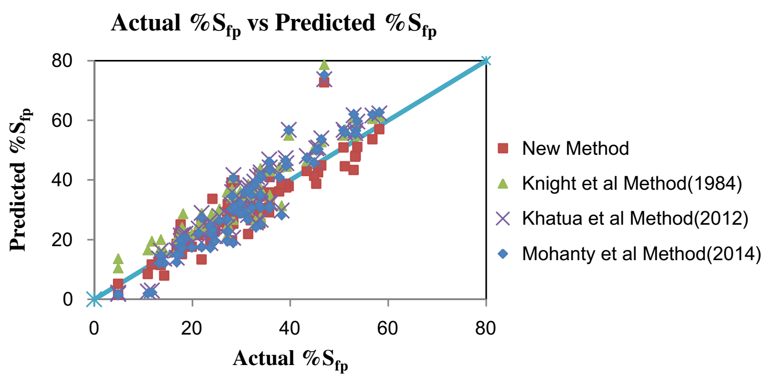

Figure 7. Scatter plot for observed and modeled value of $\%S_{fp}$.

channels. Figure (4) shows the variation in $\%S_{fp}$ with relative flow depths β for each channel for different converging angles θ. From the figure it is seen that $\%S_{fp}$ increases with increase in relative flow depth. Similarly, the variations in $\%S_{fp}$ with relative distance X_r are plotted for different relative depths in Figure (5). From the Figure (5) it is seen that the shear force percentage carried by flood plains ($\%S_{fp}$) is found to decrease from section to section of all the converging compound channels

Table 2. Unstandardized coefficient and regression statistics.

Coefficients		Regression statistics	
Intercept	−22.985	Multiple *R*	0.911
β	0.767	*R* Square	0.831
X_r	0.899	Adjusted *R* Square	0.826
θ	0.281	Standard error	7.154

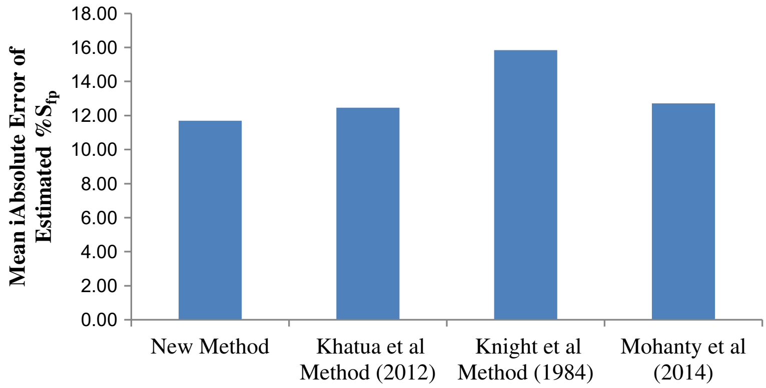

Figure 8. Mean Absolute Error by standard approaches applied to Present experimental channel data.

for all converging channels. The variation in $\%S_{fp}$ with different converging angles θ for different relative depths are also shown in Figure (6), showing an increase of shear force percentage carried by flood plains with increase in the overbank flow depth. From these graphs we observed that the $\%S_{fp}$ has power function with depth ratio (β), linear function with relative distance (X_r), and converging angle (θ), respectively, as presented in Equations (9–11).

By analyzing the above plots, percentages of boundary shear stress carried by flood plain region i.e. $\%S_{fp}$ with different non-dimensional geometric and hydraulic parameters of compound channel with converging flood plain are found to be

$$\%S_{fp} = F_1(\beta) = A(\beta)^{0.63} \tag{9}$$

$$\%S_{fp} = F_2(X_r) = B(X_r) + C \tag{10}$$

$$\%S_{fp} = F_3(\theta) = D(\theta) + E \tag{11}$$

These equations (Equations 9–11) show the relation between $\%S_{fp}$ with relative depth, converging angle, and relative distance. From the above graphs (Figure 4–6) it is also seen that R^2 value is very high and varies from 0.95 to 0.99 for each chosen functional relationships. Using the above relationships we compiled to develop a mathematical model using the regression analysis software in Micro Excel tool.

Table 2 represents the result of regression statistics, coefficients, and intercept from the linear regression analysis. After compiling all the equations (Equation 9–11) and unstandardized coefficients of Table 2, a generalized mathematical empirical relation is created and is shown in Equation 12.

$$\begin{aligned}\%S_{fp} = &-22.985 + 0.767\left(F_1(\beta)\right)\\ &+ 0.899(F_2(X_r)) + 0.281(F_3(\theta))\end{aligned} \tag{12}$$

After simplifying the above equation,

$$\%S_{fp} = 18.505 + 62.140(\beta)^{0.631} - 24.42(X_r) + 1.38(\theta) \tag{13}$$

Equation (13) represents the final expression of the model.

The variation between the calculated values of ($\%S_{fp}$) for compound channel with converging flood plain using Equations (1), (5), and (7) and the corresponding observed values for all the six types of channels are shown in Figure 7. The percentage error in the estimation of ($\%S_{fp}$) is less for model II when compared to the previous models for both Present experimental channel as well as Rezaei (2006) channels.

Using the new equation, various conventional methods are estimated for the flow cases considered in Present experimental channel of Rourkela and Rezaei (2006) channel. The methods considered are Khatua et al. (2012), Knight and Hamed (1984), Mohanty et al. (2014).The percentage of error in estimating the discharge is computed as

$$\text{Mean Absolute Error}(\%) = \frac{100\%}{N}\left|\frac{S_{fpcal} - S_{fpact}}{S_{fpact}}\right| \tag{14}$$

where S_{fpcalc} is the estimated discharge, S_{fpact} is the actual discharge, and N is the total number of data. Figure (8) shows the comparison among various methods in Present experimental channel of Rourkela and Rezaei (2006) channel cases. In Figure 8, the New Method appears to be the best method.

5. Results and discussion

5.1. Error analysis

To check the strength of the model, error analyses have been done. Mean absolute error (MAE), the mean absolute percentage error (MAPE), mean squared error (MSE), and the root mean squared error (RMSE) for all the converging compound channels for different flow conditions have been estimated. The definitions of error terms are described below. The detailed results of the error analysis have been presented in Table 3. The expression used to estimate errors in different forms are

5.1.1. Mean Absolute Error (MAE)

The Mean Absolute Error has been evaluated as,

$$\text{MAE} = \frac{1}{n}\sum_{i}^{n}\left|\frac{P_i - O_i}{O_i}\right| \tag{15}$$

Table 3. Statistical error analysis of different methods.

	Methods			
Statistical parameters	New Method	Khatua et al.	Knight et al. method	Mohanty et al. method
MSE	28.78119	35.62421	45.33	39.95373
RMSE	5.364811	5.968602	6.73	6.320896
MAE	3.734498	4.759234	5.31	4.746045
MAPE	13.43366	17.19923	21.63	17.4745

where P_i = predicted values, O_i = observed values.

5.1.2. Mean Absolute Percentage Error (MAPE)

MAPE also known as Mean absolute Percentage Deviation. It was usually expressed as a percentage, and was defined by the formula

$$\text{MAPE} = \frac{1}{n}\sum_{i}^{n}\left|\frac{O_i - P_i}{O_i}\right| \tag{16}$$

5.1.3. Mean Squared Error (MSE)

MSE measures the average of the squares of the errors. It is computed as

$$\text{MSE} = \frac{1}{n}\sum_{i}^{n}(P_i - O_i)^2 \tag{17}$$

5.1.4. Root Mean Squared Error (RMSE)

RMSE or Root Mean Squared Deviation is also a measure of the differences between values predicted by model or an estimator and the actually observed values. These individual differences are called as residuals when the calculations are performed over the data sample that is used for estimation, and are known as estimation errors when computed out of the sample. The RMSE is defined as,

$$\text{RMSE} = \sqrt{\text{MSE}} \tag{18}$$

6. Conclusions

The following conclusions can be derived from the above research presented in this work.

(1) From the experimental results on converging compound channels, the boundary shear from point to point along the wetted perimeter for different sections along the converging compound channels are measured and the distribution of shear force carried by flood plains and in main channel perimeters were presented.
(2) In all sections the boundary shear is found to be maximum at the middle of main channel and gradually decreases towards the interface between the main channel and flood plain. At the interface, the boundary shear suddenly falls then it decreases and reaches minimum at both the ends of floodplain. This may be due to momentum transfer phenomena occurring between the main channel and the flood plain.
(3) The dependency of shear force percentage carried by flood plains with five most influencing non-dimensional geometric and hydraulic parameters of a converging compound channel are evaluated and modeled. The $\%S_{fp}$ in converging compound channel is found to be a non-linear function of all these non-dimensional parameters.
(4) Different standard models to predict the shear force percentage carried by flood plains are applied to the present channel and the channels of other investigators. The present mathematical model presented for $\%S_{fp}$ of a converging compound channel gives least error when compared with other models applied at different reaches of the channels.
(5) Error analysis in terms of MSE, RMSE, MAE, and MAPE are performed for all data series by all the models to predict the shear force percentage carried by converging flood plains showing the efficacy of the present model.

Acknowledgments

The author wish to acknowledge thankfully the support from the Institute and the UGC UKIERI Research project (ref no UGC-2013 14/017) by the second authors for carrying out the research work in the Hydraulics laboratory at National Institute of Technology, Rourkela.

Disclosure statement

No potential conflict of interest was reported by the authors.

Funding

This work was supported by the Institute and the UGC UKIERI Research project [ref no UGC-2013 14/017]; National Institute of Technology Rourkela.

References

Bousmar, D., and Zech, Y. (1999). "Momentum transfer for practical flow computation in compound channels." *J. Hydraul. Eng.*, 125(7), 696–706.
Bousmar, D., Wilkin, N., Jacquemart, J.H., and Zech, Y. (2004). "Overbank flow in symmetrically narrowing floodplains." *J. Hydraul. Eng.*, 130(4), 305–312.
Ghosh, S., and Jena, S.B. (1971). "Boundary shear stress distribution in open channel compound Proc." *Inst. Civil Eng.*, 49, 417–430.
Khatua, K.K., and Patra, K.C. (2007). "Boundary shear stress distribution in compound open channel flow." *ISH J. Hydraul. Eng.*, 13(3), 39–54.
Khatua, K.K., Patra, K.C., and Mohanty, P.K. (2012). "Stage-discharge prediction for straight and smooth compound channels with wide floodplains." *J. Hydraul. Eng.*, 138(1), 93–99.
Knight, D.W., and Demetriou, J.D. (1983). "Flood plain and main channel flow interaction." *J. Hydraul. Eng.*, 109(8), 1073–1092.
Knight, D.W., and Hamed, M.E. (1984). "Boundary shear in symmetrical compound channels." *J. Hydraul. Eng.*, 110(10), 1412–1430.
Mohanty, P.K., Khatua, K.K., and Dash, S.S. (2014). "Flow prediction in two stage wide compound channels." *ISH J. Hydraul. Eng.*
Mohanty, P. K., & Khatua, K. K. (2014). "Estimation of discharge and its distribution in compound channels." *Journal of Hydrodynamics, Ser. B*, 26(1), 144–154.
Patel, V.C. (1965). "Calibration of the Preston tube and limitations on its use in pressure gradients." *J. Fluid Mech.*, 231, 85–208. Cambridge University Press.
Patra, K.C., Kar, S.K., and Bhattacharya, A.K. (2004). "Flow and velocity distribution in meandering compound channels." *J. Hydraul. Eng.*, 130(5), 398–411.

Proust, S., Rivière, N., Bousmar, D., Paquier, A., and Zech, Y. (2006). "Flow in compound channel with abrupt floodplain contraction." *J. Hydraul. Eng.*, 132(9), 958–970.
Rezaei, B. (2006). "Overbank flow in compound channels with prismatic and non-prismatic floodplains." PhD thesis, Univ. of Birmingham, UK.
Sellin, R.H.J. (1964). "A laboratory investigation into the interaction between the flow in the channel of a river and that over its flood plain." *La Houille Blanche*, 7, 793–802.